ISBN: 978-3-95450-184-7 doi:10.18429/JACoW-IPAC2018-MOPMF004

SPIN DYNAMICS IN THE JLEIC ALTERNATIVE PRE-BOOSTER RING*

J. Martinez-Marin[1], B. Mustapha, Argonne National Laboratory, 60439 Chicago, USA
[1]also at Illinois Institute of Technology, 60616 Chicago, USA

Abstract

In order to reduce the foot-print of the JLEIC ion complex, we have designed a more compact and cost-effective octagonal 3-GeV pre-booster ring half the size of the original figure-8 design. However, this new ring does not preserve ion polarization by design as the figure-8 shape, making it necessary to study the spin dynamics to find the best solution for spin correction. Different codes, Zgoubi [1] and COSY [2], are used to model and simulate the spin dynamics in the octagonal 3 GeV ring, including spin correction with Siberian snakes.

INTRODUCTION

In an effort to lower the risk and reduce the footprint of the JLEIC ion accelerator complex, an alternative design approach has been proposed [3]. An essential part of the alternative approach is to replace the 8-GeV figure-8 booster of the current baseline design [4] with a more compact 3-GeV pre-booster ring and to use the electron storage ring (e-ring) as a large ion booster up to 16 GeV.

JLEIC Alternative Ion Complex Design

The layout of the proposed alternative design is shown in Fig. 1. It consists mainly of [3]:

- A more compact 130 MeV linac [4].
- A more compact 3-GeV pre-booster using RT magnets [5]. At this energy, the figure-8 shape is not required, a different mechanism with reasonable magnetic fields could be used for spin corrections.
- The e-ring as a large ion booster, up to 16 GeV protons with new magnets instead of PEP-II magnets.

In the e-ring, the figure-8 shape preserves the ion spin by design, but it is necessary to study the spin dynamics in the pre-booster, in order to investigate depolarization effects and develop an appropriate spin correction scheme. The goal is to preserve at least 70% of ion spin polarization at the interaction point.

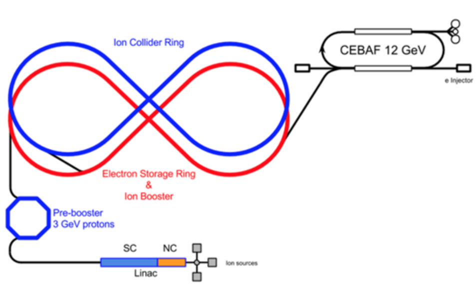

Figure 1: Layout of the alterati ve JLEIC design.

*This work was supported by the U.S. Department of Energy, Office of Nuclear Physics, under Contract No. DE-AC02-06CH11357

The Compact Pre-Booster Ring

The 8-GeV booster in the current baseline design has been replaced by a more compact 3-GeV pre-booster ring (Fig. 2). Table 1 shows the design parameters for the proposed octagonal design [7].

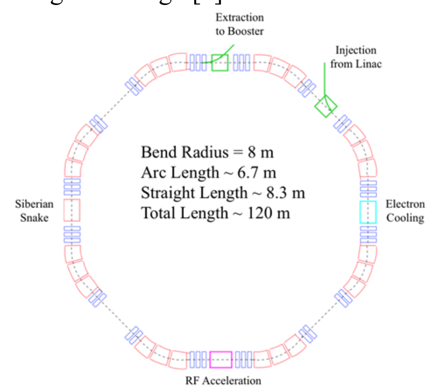

Figure 2: Layout of the octagonal pre-booster design.

This design has a circumference of 120 m with four dispersive and four non-dispersive straight sections. The four dispersion-free sections will be used for rf acceleration, electron cooling, spin correction and beam extraction to the e-ring serving as a large ion booster. One of the dispersive sections is used for injection from the linac while other sections will be used for higher order corrections [6]. The non-dispersive section reserved for spin correction is about 4 meters long.

Table 1: Design Parameters of the 3-GeV Pre-Booster

Parameter	Octagonal
Circumference, m	120
Maximum β_x , m	15.3
Maximum β_y, m	21
β_x at injection, m	6.0
β_y at injection, m	11.2
α_x, α_y at injection	0
Maximum dispersion, m	4.2
Normalized dispersion at injection	1.7
Tune in X	3.01
Tune in Y	1.18
Transition γ	4.7
Momentum compaction factor	0.045

The pre-booster energy range is 130 MeV/u – 3 GeV/u for protons, 75 MeV/u – 1.2 GeV/u for deuterons and 40 MeV/u - 610 MeV/u for lead ions.

ISBN: 978-3-95450-184-7 doi:10.18429/JACoW-IPAC2018-MOPMF004

SPIN DYNAMICS

A study of the spin dynamics in the 3-GeV octagonal pre-booster for both protons and deuterons has been carried out. In all simulations, an energy ramping rate of ~ 36 keV/turn and an unnormalized rms vertical emittance ($\varepsilon_{y,rms}$) of 6 π mm.mrad were used. The spin particles are launched onto the closed orbit. Momentum offset was not included in this study, but it will be added in the future to consider the effect of synchrotron sideband resonances.

Spin Resonances

The spin tune of a polarized beam is the number of spin precessions per turn. In a conventional ring: $\nu_s = G\gamma$, where ν_s is the spin tune, G is the anomalous g-factor of the beam particle and γ is the relativistic factor. For protons: G ≈ 1.793 and for deuterons: G ≈ -0.143.

A spin resonance occurs whenever the spin precession becomes synchronized with the frequency of a spin perturbing field [7]. There are different types of resonances:

- Intrinsic resonances due to betatron oscillations:

$$\nu_s = n \pm \nu_y \quad (1)$$

- Imperfection resonances due to alignment and field errors:

$$\nu_s = n \quad (2)$$

- Coupling and higher-order resonances:

$$\nu_s = n \pm l\nu_x \pm m\nu_y \pm k\nu_{syn} \quad (3)$$

where n, l, m, k are integers, ν_x, ν_y are the horizontal and vertical betatron tunes and ν_{syn} is the synchrotron tune.

We notice a clear distinction in spin dynamics between protons and deuterons in the pre-booster:

- The proton spin is subject to several resonances as listed in Tables 2, 3, 4 and shown in Figures 3, 4. The weak intrinsic resonances, $\nu_s = n \pm \nu_y$, are not included in the tables because they are very weak.
- No resonances were observed for the deuteron spin due to its small anomalous g-factor G and the energy range in the pre-booster. The first deuteron resonance is expected around γ ~ 7 or 5.6 GeV/u.

Table 2 presents a summary of the numbers and types of spin resonances for protons and deuterons

Table 2: Types & Numbers of Spin Resonances

Resonance	Proton	Deuteron
Regular Intrinsic	3	0
Weak Intrinsic	8	0
Imperfection	5	0

Table 3 lists the intrinsic spin resonances observed for a perfect ring lattice, while figure 3 shows their strengths.

Table 3: Intrinsic Resonances for Protons

Resonance	Gγ	KE (MeV)
Intrinsic	$nP - \nu_z$ $4 - \nu_z = 2.82$	538
Strong Intrinsic	$nP + \nu_z$ $4 + \nu_z = 5.18$	1773
Very Strong Intrinsic	$nPM - \nu_z$ $8 - \nu_z = 6.82$	2631

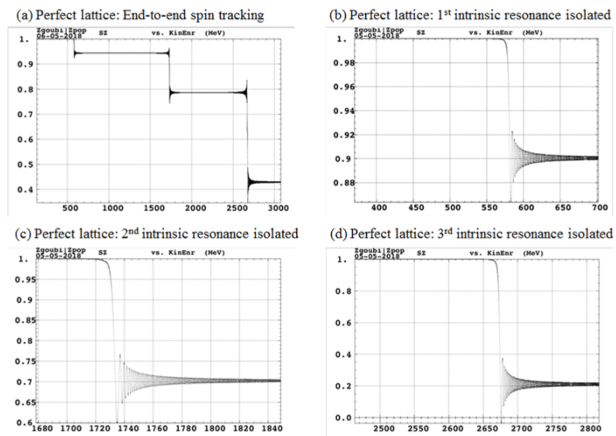

Figure 3: Vertical spin component S_y vs. proton kinetic energy KE (MeV) for a perfect pre-booster lattice showing the energy location (a) and the strengths of three intrinsic resonances (b-d). Results obtained with Zgoubi code for $\varepsilon_{y,rms}$= 6π mm.mrad.

In order to calculate imperfection resonances, errors must be added to the ring. Figure 4 shows the effect of adding a kicker to simulate a dipole field error of ~ 1%, which increases the orbit distortion. Table 4 lists the imperfection resonances observed in this case. It is worth noting that similar results were obtained by adding misalignment errors of ~ 1 mm for position and 2 mrad for angle, quadrupole field errors and higher order sextupole errors of ~ 10^{-3}.

Table 4: Imperfection Resonances for Protons

Resonance	Gγ	KE (MeV)
Regular	k = 3	632
Very Strong	kP = 4	1155
Regular	k = 5	1678
Regular	k = 6	2202
Regular	k = 7	2725

Where P = 4 is the number of super-periods and M = 2 is the number of cells per super-period.

ISBN: 978-3-95450-184-7 doi:10.18429/JACoW-IPAC2018-MOPMF004

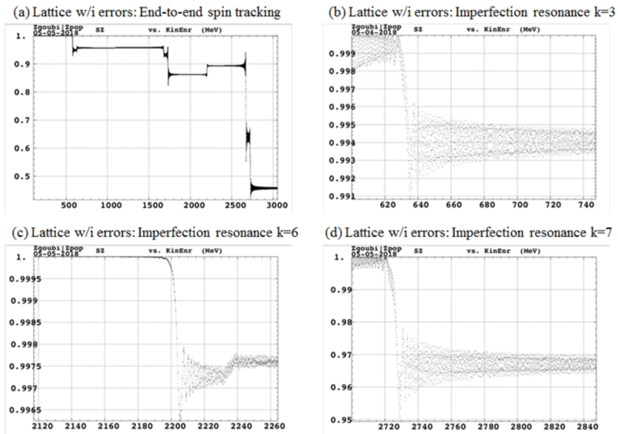

Figure 4: S_y vs KE (MeV) for the pre-booster with errors showing the energy location of imperfection resonances in addition to the intrinsic ones (a). Plots (b-d) show the strength of isolated imperfection resonances k=3, 6 and 7.

Strength of Spin Resonances

It is possible to determine the strength of the spin resonances by isolating them (see Figs. 3-(b-d) and 4-(b-d)) and using the *Froissart-Stora* formula [9] expressing the polarization fraction after crossing a resonance.

$$P_f / P_i = 2\exp\left(-\frac{\pi|\varepsilon|^2}{2\ \alpha}\right) - 1 \quad (4)$$

$$\alpha = G\frac{d\gamma}{d\theta} = G\frac{1}{2\pi M_0}\Delta E \quad (5)$$

where Pi and Pf are the initial and final polarizations respectively, ε is the resonance strength and α is the resonance crossing speed.

The strength of a resonance depends on the beam emittance. The following Table 5 shows how the emittance affects the spin polarization.

Table 5: 1st Intrinsic Resonance Depolarization as Function of Beam Emittance

Unnormalized rms emittance, mm.mrad	P_f/P_i
6π	0.90
10π	0.53
20π	-0.25

Examining the strength of the resonances found, it is important to notice that the weak resonances, localized at n ± ν_z, are negligible (<1% of polarization loss). Moreover, the majority of resonances found are not too strong. The main resonances of concern are the three intrinsic resonances which may cause considerable depolarization. See Table 6 and 7 for the strength of the resonances.

Table 6: Strength of Intrinsic Resonances (Proton Beam)

Resonance Strength	Gγ	P_f/P_i	ε_k
Medium	2.82	0.9	0.0006
Strong	5.18	0.7	0.0012
Very Strong	6.82	0.2	0.0019

Table 7: Strength of Imperfection Resonances (Proton Beam)

Resonance Strength	Gγ	P_f/P_i	ε_k
Negligible	3	0.9955	0.000127
Negligible	4	0.9999	0.000160
Negligible	5	0.9930	0.000158
Negligible	6	0.9975	0.000138
Weak	7	0.9675	0.000342

OPTIONS FOR SPIN CORRECTION

Based on this study, we can propose several ways to avoid depolarization, see Table 8. They are based on the number of resonances and their strengths taking into account the parameters and goals for the pre-booster: the crossing speed α = 1.1224x10^{-5} corresponding to the energy ramp rate, the space available spin for correcting elements and at least 70% polarization required at the interaction point.

Although it is possible, the Pulsed Quads option is not recommended for intrinsic resonances because of potential beam emittance growth. For the Siberian Snake option [10], the space requirement is still under investigation.

Siberian Snake

There is no space for a full Siberian snake. From Fig. 5, it can be concluded that a 5% Snake is needed in order to avoid the imperfection resonances, and at least a 36.5% snake is required to overcome all resonances.

- 5% Solenoid [7] for imperfection resonances:

$$\int B_{\parallel} dl = \frac{\pi}{1+G} B\rho = \frac{10.479}{1+G} p \left[\frac{GeV}{c}\right] \quad (6)$$

  4.6898 Tm with a field of 1.5 T, it will need less than 3.5 m long.
- 40% Modified Steffen Snake [7] for all resonances: in order to minimize the maximum orbit excursion more than 4.5 m long is needed.

Table 8: Overcoming the Pre-Booster Depolarizing Resonances for Proton Beams

Option	~ 5 Imperfection	~ 2 Strong Intrinsic	~ 1 Intrinsic	~ 8 Weak Intrinsic
A	Orbit corrections	Rf Dipole	Rf Dipole	Nothing/Pulsed Quads
B	5% Siberian Snake	Rf Dipole	Rf Dipole	Nothing/Pulsed Quads
C	Orbit Correction	Pulsed Quads	Pulsed Quads	Nothing/Pulsed Quads
D	5% Siberian Snake	Pulsed Quads	Pulsed Quads	Nothing/Pulsed Quads
E	40% Siberian Snake	40% Siberian Snake	40% Siberian Snake	40% Siberian Snake

ISBN: 978-3-95450-184-7 doi:10.18429/JACoW-IPAC2018-MOPMF004

CONCLUSIONS

A Siberian Snake would be the best option to avoid depolarization if space is available. In our case, neither a full Siberian Snake nor a 40% snake can be used due to lack of space. There is enough room for a 5% Steffen Snake or a 5% solenoid to correct imperfection resonances. Using a partial Siberian snake will also require spin matching at injection and extraction. A helical Snake [11] can be a solution for all resonances because it is more compact but will require detailed 3D modeling. Using an rf Dipole [12] could be enough to avoid the strong intrinsic resonances and minimize depolarization.

Although the results presented here are from Zgoubi simulations, the same results regarding the energy locations and the number of intrinsic resonances were also obtained with COSY.

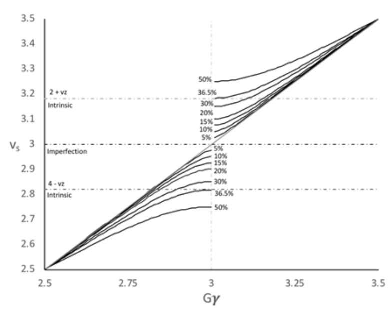

Figure 5: Spin tune vs Gγ showing the spin tune gap/jump required to avoid the resonances.

REFERENCES

[1] F. Méot, “ZGOUBI users’ guide”, C-AD/AP/470, Brookhaven National Laboratory, Upton, 2013

[2] M. Berz and K. Makino, “COSY INFINITY 9.1 programmer’s manual”, MSUHEP 101214, Michigan State University, East Lansing, 2011, http://cosyinfinity.org

[3] B. Mustapha *et al.*, “An Alternative Approach for the JLEIC Ion Accelerator Complex”, *Proc. NA-PAC’16*, Chicago, IL, October 2016, paper TUPOB05, p. 486.

[4] V. Morozov, “Overview of Jefferson Lab EIC Design and R&D”, *Proc. NA-PAC’16*, Chicago, IL, October 2016, paper MOB2IO02.

[5] J. Breitschopf *et al.*, “Superferric arc dipoles for the Ion Ring and Booster of JLEIC”, *Proc. NA-PAC’16*, Chicago, IL, October 2016, paper MOPOB54.

[6] P. Ostroumov *et al.*, “Design and Beam Dynamics Studies of a Multi-ion Linac Injector for the JLEIC Ion Complex”, *Proc. HB’16*, Malmo, Sweden, July 2016, paper THPM5Y01, p. 559.

[7] B. Mustapha, P.N. Ostroumov and B. Erdelyi, “A More Compact Design for the JLEIC Ion Pre-Booster Ring”, *Proc. NA-PAC’16*, Chicago, IL, October 2016, paper TUPOB04, p. 483.

[8] S.Y. Lee, Spin Dynamics and Snakes in Synchrotron, World Scientific Pub. Co., Singapore, 1997.

[9] M. Froissart and R. Stora, “Depolarisation d'un faisceau de protons polarisds dans un synchrotron”, *Nucl. Instrum. Methods* **7**, p. 297, 1960.

[10] Ya.S. Derbenev and A. M. Kondratenko, Part. Accel. B, 115, 1975.

[11] V. I. Ptitsin and Y. M. Shatunov, “Helical Spin rotators and snakes”, *Proc. Third Workshop on Siberian Snakes and Rotators*, Upton, NY, 1994, Brookhaven National Laboratory Report BNL-52453.

[12] M. Bai *et al.*, “Overcoming intrinsic spin Rresonances with an RF dipole”, Phys. Rev. Lett. **80**, p. 4673, 1998.